ARAP3 is essential for formation of lamellipodia after growth factor stimulation

Sonja Krugmann*, Simon Andrews, Len Stephens and Phillip T. Hawkins

The Inositide Laboratory, The Babraham Institute, Cambridge, CB2 4AT, UK
*Author for correspondence (e-mail: sonja.krugmann@bbsrc.ac.uk)

Summary

Rho and Arf family small GTPases control dynamic actin rearrangements and vesicular trafficking events. ARAP3 is a dual GAP for RhoA and Arf6 that is regulated by phosphatidylinositol (3,4,5)-trisphosphate [PtdIns(3,4,5)P_3], a product of the phosphoinositide 3-kinase (PI3K) signalling pathway. To investigate the physiological function of ARAP3, we used an RNAi-based approach in an endothelial cell model. ARAP3-deficient cells showed increased activities of RhoA and Arf6. Phenotypically, they were more rounded than control counterparts and displayed very fine stress fibres. ARAP3-deficient cells were not capable of producing lamellipodia upon growth factor stimulation, a process known to depend on PI3K and Rac activities. Rac was transiently activated in stimulated ARAP3 RNAi cells although its cellular localisation was altered, a likely consequence of increased Arf6 activity. We conclude that ARAP3 recruitment to sites of elevated PtdIns(3,4,5)P_3 is crucial to allow localised inactivation of RhoA and cycling of Arf6, both of which are necessary to allow growth factor-stimulated formation of lamellipodia.

Supplementary material available online at
http://jcs.biologists.org/cgi/content/full/119/3/425/DC1

Key words: GTPase-activating protein, ARAP3, PI3K, Rho, Arf, Lamellipodium

Introduction

Many cells respond to appropriate signals by forming lamellipodia, dynamic, sheet-like membrane protrusions containing a highly branched actin meshwork. Lamellipodia are points for insertion of new membrane components and enriched in many signalling molecules. Migrating cells form lamellipodia at their leading edges; new points of adhesion to the substratum are continuously being built at the leading edge, and together with detachment at the rear this causes net cell movement (Small et al., 2002; Ridley et al., 2003).

The signalling molecules involved in the regulation of lamellipodium formation have been studied intensively. Critically important to the mechanism of lamellipodium formation is the opposing action of the small GTPases RhoA and Rac. Small GTPases (Takai et al., 2001) act as molecular switches. They are active, and can signal to downstream effectors but only when bound to GTP. Through their intrinsic GTPase activity, small GTPases switch off by converting this GTP to GDP. Under cellular conditions the intrinsic rate of exchange of bound nucleotide is low and small GTPases are activated by factors accelerating nucleotide exchange (GEFs) and inhibited by factors enhancing their GTPase activity (GAPs).

The Rho family small GTPase Rac is necessary for receptor activation of normal, protrusive lamellipodia formation, and sufficient when activated, to cause uniform membrane ruffling along the entire edge of the cell (Ridley and Hall, 1992). By contrast, activation of RhoA stimulates the formation of retractile actomyosin stress fibres and focal adhesions (Ridley et al., 1992). This, in turn, causes increased contractility across

the cell, particularly important for retraction at the rear of the motile cell. RhoA and Rac effectively counteract each other. Inhibition of RhoA by C3 transferase increases membrane ruffling (Rottner et al., 1999) and locally RhoA effectively antagonises Rac-dependent lamellipodium formation (Worthylake and Burridge, 2003). In neutrophils establishing polarity, there is high Rac and low Rho activity at the leading edge and the opposite at the rear (Xu et al., 2003).

Arf6, an Arf family small GTPase, has also been shown to be involved in membrane ruffling and/or lamellipodium formation. There is substantial evidence that its role may be indirect, by controlling the distribution and activation status of Rac in the cell (Radhakrishna et al., 1999; Boshans et al., 2000; Franco et al., 1999). Thus, in several studies Arf6-GDP is found in an endosomal recycling compartment, that also contains Rac and upon activation of Arf6 these recycling endosomes fuse with the plasma membrane. Interestingly, activation of Arf6 can occur through receptor- and PI3K-dependent activation of certain cytohesin family Arf GEFs (Venkateswarlu and Cullen, 2000), which this model would predict enables delivery of new membrane and Rac to sites of PI3K (and hence Rac) activation. However, this model is still uncertain, as in several other studies Arf6-GDP has also been found at the plasma membrane (Cavenagh et al., 1996; Altschuler et al., 1999; Macia et al., 2004) and hence Arf6 may also have Rac-independent roles in the regulation of lamellipodium formation.

Agonist-stimulated PI3Ks are responsible for the generation of the lipid second messenger PtdIns(3,4,5)P_3 at the cytosolic face of the plasma membrane (Vanhaesebroeck et al., 2001).

PI3Ks are known to be important for lamellipodium formation following receptor stimulation (Wennström et al., 1994). At least one role for PtdIns(3,4,5)P_3 in this process is likely to be the activation of Rac (Hawkins et al., 1995; Reif et al., 1996). Although there are also PI3K-independent mechanisms that can lead to the activation of Rac (Nobes et al., 1995; Akasaki et al., 1999), it remains true that the large majority of agonists that can activate lamellipodia formation do so via a PI3K and Rac dependent mechanism. Several Rac GEFs have been described that can be activated by PtdIns(3,4,5)P_3 (Welch et al., 2002) and could mediate PI3K-dependent activation of Rac and of lamellipodium formation.

ARAP3 is a dual GAP protein containing five PH domains. We have shown previously that ARAP3 translocates to PtdIns(3,4,5)P_3-containing membranes and that it acts as a PtdIns(3,4,5)P_3-dependent Arf6 GAP and a PI3K- and Rap-activated RhoA GAP (Krugmann et al., 2002; Krugmann et al., 2004). Overexpression of ARAP3 in PAE cells has a dramatic effect on the actin cytoskeleton leading to PDGF-induced cell retractions and loss of adhesion. The aim of the work described here was to assess the role of endogenous ARAP3 in PAE cells using RNAi technology.

Results
Generation of ARAP3-knockdown PAE cell lines
We have previously shown that ARAP3 is broadly expressed in many tissues and a number of cell lines; expression was high in PAE cells and overexpression of ARAP3 in PAE cells caused PDGF-dependent retractions as opposed to lamellipodia formation (Krugmann et al., 2002; Krugmann et al., 2004). To better understand the physiological role of ARAP3, we decided to deplete PAE cells of ARAP3. We designed five RNAi oligos to knock down porcine ARAP3. Two oligos, which proved most effective in transient transfection assays were used to generate stable, clonal PAE cell lines. For each RNAi vector, 50 clonal lines were screened for endogenous ARAP3 expression by immunoblotting. Most of the experiments presented in this report were obtained with the experimental cell line, 52B3, showing approximately 85% knock down of ARAP3 levels (Fig. 1A) and a single control RNAi expressing cell line (NA1), both of which grew well in culture. Key results are reproduced with an independent experimental cell line, 32D6, derived from an alternative RNAi oligo to that used to generate 52B3 (Fig. 1A). PAE cells expressing control RNAi did not differ significantly from the parental PAE cells in any of the experiments performed (not shown).

ARAP3-knockdown cells have a characteristic phenotype
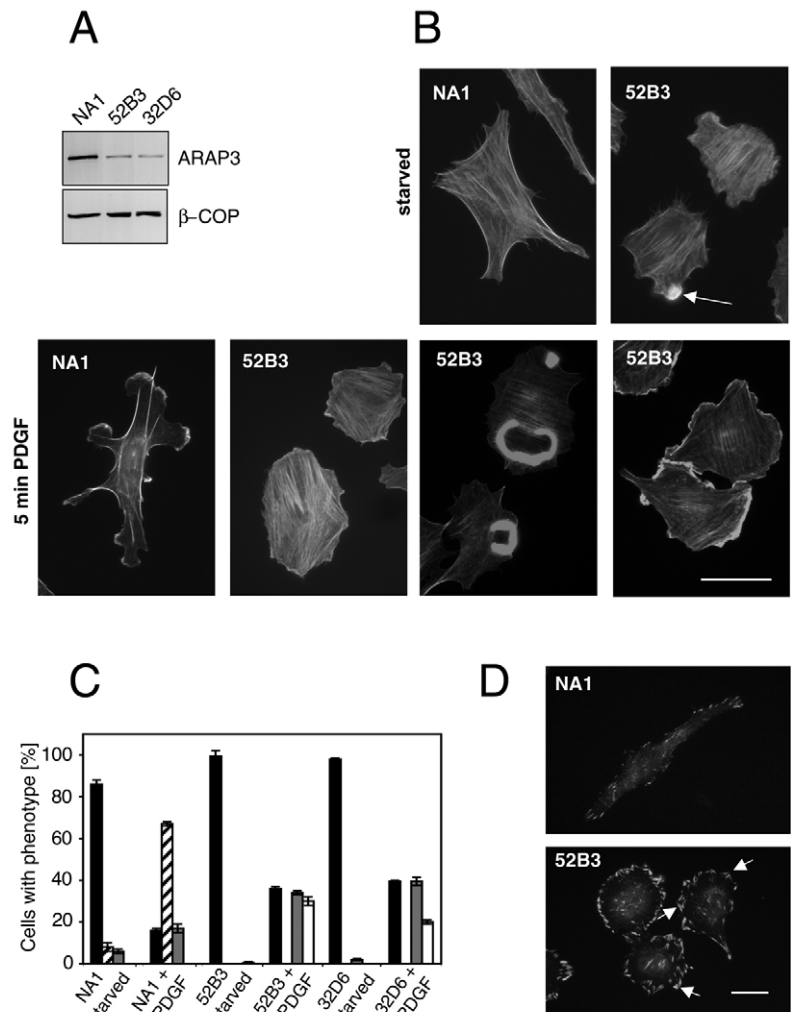In the context of our earlier work describing the impact of

Fig. 1. ARAP3-deficient cells do not form protrusive lamellipodia. (A) Western blots of lysates of stable PAE cell lines expressing a scrambled control RNAi oligonucleotide (clone NA1) or olignucleotides directed against different parts of porcine ARAP3 (clones 52B3, 32D6) were probed for ARAP3 (top panel) and subsequently reprobed for β-COP as a loading control (bottom panel). Careful analysis of blots from several similar experiments leads us to estimate that the reduction in ARAP3 expression in the 52B3 and 32D6 lines is approximately 85%. The original blot had 25 lanes, out of which the shown ones were not immediately adjacent. They were cut and pasted for ease of viewing. (B) Cells of the stable RNAi PAE cell lines were seeded onto coverslips, starved for 16 hours, stimulated for 5 minutes either with PDGF or with its vehicle (as indicated) and fixed. Cells were stained for F-actin. An arrow points to a 52B3 cell carrying a typical small actin-rich protrusion. The photographs shown are representative examples from four independent experiments. (C) NA1, 52B3 and 32D6 cells were treated as above and 120-150 cells per coverslip were counted and scored according to their phenotypes: black bars, no ruffles or lamellipodia; striped bars, protrusive lamellipodia; grey bars, uniform ruffles along entire cell periphery; unfilled bars, dorsal ring ruffles. (D) NA1 and 52B3 cells were treated as in (B) and stained for paxillin. Arrows point to typical clustered focal adhesions in 52B3 cells. Bars in (B) and (D), 20 μm.

overexpressing ARAP3 on PAE cells (Krugmann et al., 2002; Krugmann et al., 2004) we examined the effect of knockdown of ARAP3 on the actin cytoskeleton in serum-starved and PDGF-stimulated PAE cells. We found both 52B3 and 32D6 cells displayed a number of dramatic changes compared with

NA1 control cells. The phenotypic changes (see below) diminished with increasing passage number and were very clear only for the first five passages, indicating the cells underwent compensatory changes. Serum-starved ARAP3-deficient cells were significantly more rounded than control cells (Fig. 1B; Fig. S1A, supplementary material). 46% of the starved 52B3 cells (and 36% of 32D6 cells) displayed at least one small actin-rich protrusion (see arrow), which was reminiscent of those seen in wild type or constitutively active Arf6-overexpressing cells (see below) (Radhakrishna et al., 1999; Boshans et al., 2000; Santy, 2003). ARAP3-deficient cells also contained large numbers of very fine, parallel running F-actin fibres which typically ran in several orientations, as opposed to fewer, thicker actin cables in control cells. Upon stimulation with PDGF (Fig. 1B; Fig. S1A, supplementary material), NA1 cells exhibited the dramatic changes in the actin cytoskeleton previously described for PAE cells (Wennström et al., 1994). These included a transient reduction in actin cables and the formation of large protrusions carrying lamellipodia and localised edge ruffling. By contrast, stimulating 52B3 or 32D6 cells with PDGF did not lead to significant reductions in internal stress fibres and these cells did not form lamellipodia. Instead, 36% of 52B3 (40% of 32D6) cells displayed no apparent change, 34% of 52B3 (40% of 32D6) cells displayed some edge ruffling along the entire periphery of the cell and 30% of 52B3 (20% of 32D6) cells displayed striking dorsal ruffles. (Fig. 1B,C; Fig. S1A, supplementary material). We concluded ARAP3 RNAi cells were incapable of producing PDGF-induced lamellipodia.

In addition to this striking phenotype, we observed ARAP3 RNAi cells were characterised by enlarged, and often clustered (small arrows) focal adhesions when staining with paxillin (Fig. 1D; Fig. S1B, supplementary material), vinculin or phosphotyrosine (not shown). This was most apparent in starved cells, where control RNAi cells possess only very sparse focal adhesions. Furthermore, consistent with their inability to create lamellipodia when stimulated with PDGF, ARAP3 RNAi cells also did not alter their focal adhesions in response to PDGF, while control RNAi cells displayed small focal contacts along the edge of protrusions (not shown).

The inability of ARAP3 RNAi cells to assemble lamellipodia was also reflected in the response of 52B3 and 32D6 cells in 'wound-healing' experiments, which test the ability of cells in a monolayer to polarise and move as a sheet. Time-lapse microscopy (not shown) revealed PAE cells expressing control RNAi moved in a very organised fashion as a sheet. By contrast, ARAP3-deficient cells reoccupied the available space in a less organised fashion. More specifically, we looked at three previously characterised parameters of cells moving in an organised fashion as a monolayer: (1) filamentous actin (lamellipodia) at the leading edge; (2) alignments of microtubules into the forming protrusions, thus allowing effective transport to the leading edge; and (3) 'polarisation' of the Golgi apparatus into the direction of the 'wound'. NA1 cells organised protrusions carrying lamellipodia, which linked up neighbouring cells at the leading edge, while 52B3 (and 32D6) cells did not form protrusions carrying lamellipodia at their leading edge (Fig. 2A; Fig. S2A, supplementary material). Reorganisation of the micotubules into the protrusions perpendicular to the direction of the wound edge was very obvious in NA1 cells three hours after scratching but it was
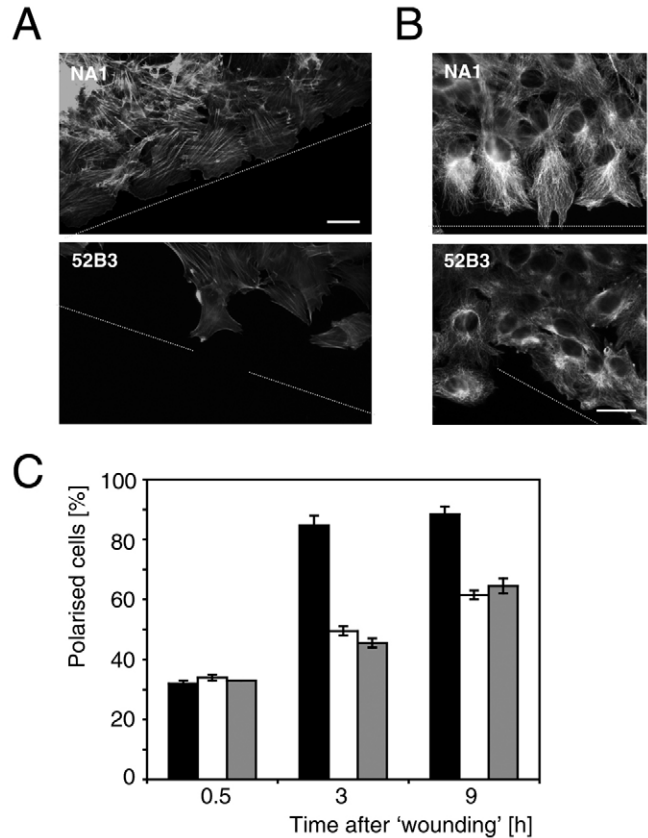
Fig. 2. ARAP3-deficient cells do not polarise well. NA1 or 52B3 cells were seeded onto coverslips and left to grow until confluent. Confluent monolayers were scratched with a sterile pipette tip and left to migrate to close the 'wound'. (A) Cells were fixed 4.5 hours after scratching, and stained to visualise F-actin. (B) Cells were fixed 3 hours after scratching and stained to visualise α-tubulin. Data similar to the photographs shown (A,B) were obtained in two further experiments. A thin broken white line indicates the orientation of the 'wound' in each photograph. Bar, 20 μm. (C) Cells were fixed 0.5, 3 and 9 hours after scratching and stained for giantin with a nuclear counterstain. Cells in which the Golgi apparatus lay within the third of the cell facing the 'wound' were counted as polarised. Black bars, NA1 control cells; unfilled bars, 52B3; grey bars, 32D6 ARAP3 RNAi cells. The graph integrates data from three independent experiments.

severely delayed and reduced in 52B3 and in 32D6 cells (Fig. 2B; Fig. S2B, supplementary material). At 9 hours after scratching, ARAP3 RNAi cells were no longer distinguishable from control RNAi cells with regard to their microtubular arrangements (not shown). Finally, re-orientation of the golgi apparatus from a random juxtanuclear position into the third of the cell that faces the wound edge (polarisation) was again significantly delayed in 52B3 and in 32D6 cells as compared with NA1 cells (Fig. 2C). We concluded ARAP3-deficient cells were also impaired in forming protrusions and polarising in the context of a wound-healing assay.

The ARAP3-knockdown phenotype can be rescued and mimicked

To test whether the observed phenotype of ARAP3 RNAi cells was indeed due to reduced ARAP3 levels, we attempted to

reverse it by transient over-expression of human ARAP3 (hARAP3). We could successfully over-express GFP-hARAP3 in both NA1 and 52B3 cells (not shown), but transiently transfected cells showed the ARAP3 overexpression phenotype, which we have previously described (i.e. loss of adhesion and PDGF-dependent cell retractions) (Krugmann et al., 2002). To allow more precise titration of expression levels, we microinjected 52B3 cells with a hARAP3-expression

Fig. 3. The ARAP3-knockdown phenotype can be rescued and mimicked. (A) 52B3 cells were seeded onto glass coverslips, starved for 16 hours and then microinjected with the injection marker biotin-dextran and pCMV3(EE) (dextran) or with biotin-dextran and pCMV3(EE)hARAP3 (hARAP3). Where indicated, cells were stimulated with PDGF for 5 minutes prior to fixation. Cells were stained for the presence of the injection marker (not shown), for F-actin (left) or for paxillin (right). The rescue result shown was observed in three independent experiments in 35% of ARAP3-injected cells. 45% of hARAP3-injected cells displayed the ARAP3-overexpression phenotype with retractions and loss of adhesion that has been previously described (Krugmann et al., 2004). (B) PAE cells were transiently transfected with pcDNA3-HA-L67Arf6 and/or pRK5-Myc-L63RhoA and the empty vector where applicable, and seeded onto glass coverslips. Cells were serum-starved for 16 hours prior to stimulation with PDGF for 5 minutes or its vehicle (indicated PDGF and starved). Cells were fixed and stained for the HA and Myc epitope tags (not shown; in cells co-transfected with Arf6 and RhoA constructs, in excess of 90% of cells expressed both plasmids if they expressed L67Arf6) or for the HA or Myc epitope tag together with filamentous actin. Arrows indicate Arf6-typical, actin-rich protrusions. The shown cells are representative examples; experiments were repeated three times. Bars, 20 μm.

plasmid or an empty control plasmid together with an expression marker and stained microinjected cells for F-actin or paxillin. While starved control-injected cells displayed the 52B3 phenotype (Fig. 3A) and strongly hARAP3-expressing cells again showed an overexpression phenotype (not shown), weakly hARAP3 expressing cells (35% of hARAP3-injected cells) showed a reversal of the knockdown phenotype with respect to their cell shape, number and thickness of stress fibres. Upon challenge with PDGF, control injected 52B3 cells were unable to form lamellipodia, while weakly hARAP3-expressing cells had regained that ability. Finally, we observed a reduction in number and thickness of focal adhesions when comparing hARAP3 injected cells with control injected counterparts (Fig. 3A).

We tried to dissect the contributions to the observed ARAP3 RNAi phenotype made by the individual catalytic activities of ARAP3 by expressing hARAP3 point mutants. However, these experiments were abandoned due to technical difficulties encountered in accurately controlling expression levels and consequent ambiguities in interpretation.

Instead, to understand the relative roles of RhoA and Arf6 regulation in the ARAP3 RNAi phenotype, we expressed constitutively active mutants of RhoA and Arf6 alone or together in normal PAE cells and compared their effects on F-actin as well as the ability of the expressing cells to produce lamellipodia after stimulation with PDGF (Fig. 3B). Co-expression of constitutively active RhoA (Myc-L63RhoA) and Arf6 (HA-L67Arf6) effectively mimicked the observed ARAP3 RNAi phenotype (Fig. 3B). Starved L67Arf6 + L63RhoA cells, like ARAP3-knockdown cells, displayed a more rounded shape than control cells; they contained multiple, thin stress fibres running in more than one orientation. In response to challenge with PDGF, L63RhoA + L67Arf6-expressing cells, like ARAP3 RNAi cells, did not undergo dramatic shape changes nor produce lamellipodia but ruffles were seen in 35% of L67Arf6 + L63RhoA expressing cells. By contrast, starved cells expressing L63RhoA (Fig. 3B) or ROCK kinase (not shown) together with an empty vector, contained thick actin cables, which ran parallel in one predominant orientation; these cells were generally rounded. L63RhoA expressing cells did not form lamellipodia nor did they ruffle upon stimulation with PDGF (Fig. 3B). Starved cells expressing L67Arf6 together with an empty vector were more elongated and contained few actin cables; as observed in the ARAP3 RNAi cells, L67Arf6-expressing cells contained frequent actin-rich membrane protrusions (arrow). When stimulated with PDGF, L67Arf6-expressing cells did not produce lamellipodia (Fig. 3B); 25% of L67Arf6 cells displayed some ruffling. Since L67Arf6, which is locked in the GTP-bound state, is often criticised as a poor model of constitutively active Arf6 with the potential to produce artefacts (Donaldson, 2003), we analysed also PAE cells expressing an empty vector together with a fast cycling Arf6 mutant (T157A) as an alternative model of increased Arf6 activity (Santy, 2003). These cells again displayed very few actin cables when starved; again actin-rich protrusions were observed. In roughly 50% of T157A Arf6-expressing cells, juxtanuclear vacuoles (see also below and Fig. 5) were observed that were enriched in F-actin. PDGF challenge of T157A Arf6 cells did not produce lamellipodia, but in 20% of PDGF-stimulated cells, ring ruffles were observed (Fig. 3).
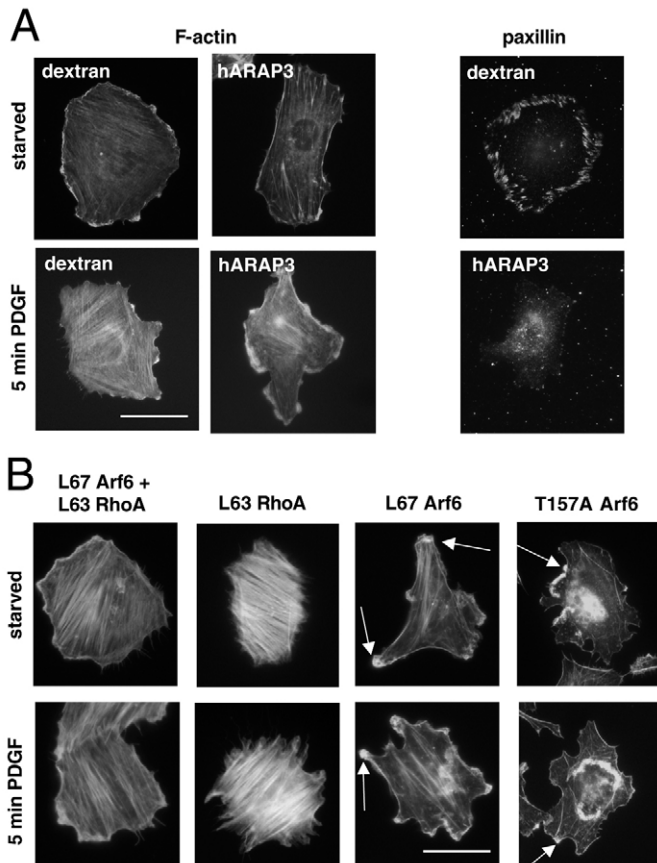
Hence, ARAP3 RNAi cells can be rescued by careful heterologous expression of ARAP3. Moreover, the observed phenotype can be mimicked by simultaneous expression of constitutively active Arf6 and RhoA constructs. Dissection of their individual phenotypes indicates the ARAP3 RNAi phenotype contains contributions from both proteins.

ARAP3-knockdown cells have increased RhoA activity

We attempted to analyse the impact of ARAP3 knockdown on the activity of RhoA. Direct quantitative assessment of RhoA activity was hindered by the fact that the antibody routinely used for RhoA 'pull-down' assays recognised porcine RhoA too poorly to be used for this purpose (not shown). We therefore used indirect measures of RhoA activity. ROCK is a direct target of RhoA known to control stress fibre formation (Leung et al., 1996; Amano et al., 1997). We measured the in vitro kinase activity of ROCK immunoprecipitates prepared from 52B3 and NA1 cells stimulated with PDGF. This revealed that in cells with reduced ARAP3, PDGF stimulated a much greater transient activation of ROCK kinase than in cells expressing control RNAi (Fig. 4A). Secondly, we looked at the myosin binding subunit (MYPT) of myosin light chain phosphatase, which is phosphorylated and inhibited by ROCK. We determined the phosphorylation status of MYPT using a phosphorylation site-specific antibody. After serum starvation, MYPT in cells with reduced levels of ARAP3 was significantly more basally phosphorylated. Furthermore, stimulation with PDGF resulted in a substantially greater rise in phosphorylation of MYPT in cell lines with reduced ARAP3 compared with controls (Fig. 4B). While it is known that the phosphorylation site seen by the anti phospho-MYPT antibody can also be regulated by kinases other than ROCK and hence cannot be assumed to be a pure read-out of Rho activity, together our results indicate that in ARAP3-deficient cells there is substantially increased Rho signalling activity, under both basal and PDGF-stimulated conditions.

ARAP3-knockdown cells have increased Arf6 activity

We also quantified the impact of ARAP3-deficiency on Arf6 signalling in PAE cells. Using a well-characterised Arf-selective bait and an Arf6-specific antibody in pull-down experiments, we recovered more Arf6-GTP from both serum starved and growing cell lines deficient in ARAP3 compared with controls (Fig. 5A). Further experiments revealed that total cellular Arf6-GTP levels in serum-starved control cells did not significantly change in response to PDGF, while cells deficient in ARAP3 responded with a significant but transient rise in Arf6-GTP (Fig. 5B).

Since PDGF stimulation, which leads to PtdIns(3,4,5)P_3 formation (Donaldson, 2003), causes the localised activation of both cytohesin-family Arf6 GEFs (Venkateswarlu and Cullen, 2002) and the Arf6 GAP ARAP3 (Krugmann et al., 2002), together, their action allows PtdIns(3,4,5)P_3 to stimulate faster cycling of Arf6. This cycling of Arf6 is thought to control an endosomal and/or plasma membrane transport system responsible for the regulated delivery of components to emerging lamellipodia (Sander et al., 1998). One component of this system whose delivery is regulated by Arf6 is Rac (Radhakrishna et al., 1999; Boshans et al., 2000). It is not clear in PAE cells whether PI3K regulates Rac directly or indirectly via Arf6. We therefore sought to establish whether the pathway
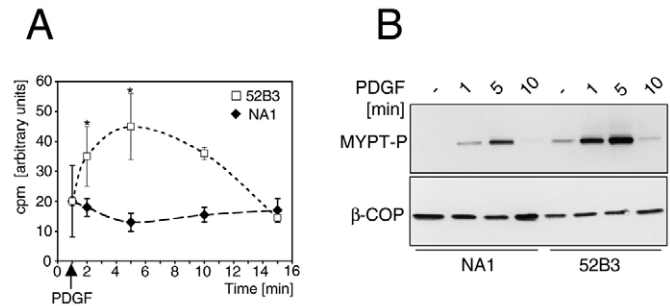

Fig. 4. ARAP3-deficient cells have increased activities of RhoA. (A) NA1 and 52B3 cells were transiently transfected with a Myc-tagged ROCK construct. After 16 hours of serum starvation, cells were or were not stimulated with PDGF or its vehicle for 1-15 minutes and lysed. ROCK protein was immunoprecipitated using an anti-Myc antibody and subsequently used for an in vitro kinase assay. The graph represents data pooled (means ± s.d.) from three independent experiments, which were all done in duplicate. The PDGF-stimulated increase in ROCK activity in the 52B3 cells is statistically significant (*P=0.05 in a paired Student's t-test). (B) NA1 and 52B3 cells were seeded into tissue culture dishes, serum starved for 16 hours and lysed straight away or after stimulation with PDGF or its vehicle for 1-10 minutes. Lysates were subjected to western blotting and probed with an anti phospho-MYPT antibody and subsequently with a control antibody (β-COP) as a loading control. The shown blot is a representative example from three independent experiments.

from PDGF-stimulation to Rac activation was compromised in ARAP3 RNAi cells.

Activation and localisation of Rac are altered in ARAP3-knockdown cells

Since it is known Arf6 controls recycling of several plasma membrane receptors, we compared initially PDGF receptor signalling in NA1 and 52B3 cells. This showed no significant difference in stimulated receptor autophosphorylation between the two cell lines (not shown), indicating that the observed defects in PDGF-stimulated changes in morphology and the actin cytoskeleton were not due to proximal defects in PDGF-receptor signalling.

We next quantified the activation status of Rac in PAE cells by a standard pull-down assay. The amount of Rac-GTP recovered from starved or growing cells did not differ significantly between ARAP RNAi and control RNAi cells (Fig. 5C). In control or ARAP3 RNAi cell lines, stimulation with PDGF resulted in a substantial but transient activation of Rac (Fig. 5D). In ARAP3-deficient cell lines the activation of Rac induced by PDGF was significantly greater at early times and declined significantly more rapidly than in control cell lines. This is consistent with the idea that more Rac may have been immediately available for activation at the cell surface but that the associated recycling of intracellular Rac to the cell surface may have been compromised in the ARAP3-deficient cell lines. Cdc42 was not affected in the ARAP3-deficient cells (data not shown).

We then compared the cellular distribution of Rac1 in control and ARAP3 RNAi cells using immunohistochemistry. As shown in Fig. 5E (top panels), Arf6 affects distribution of
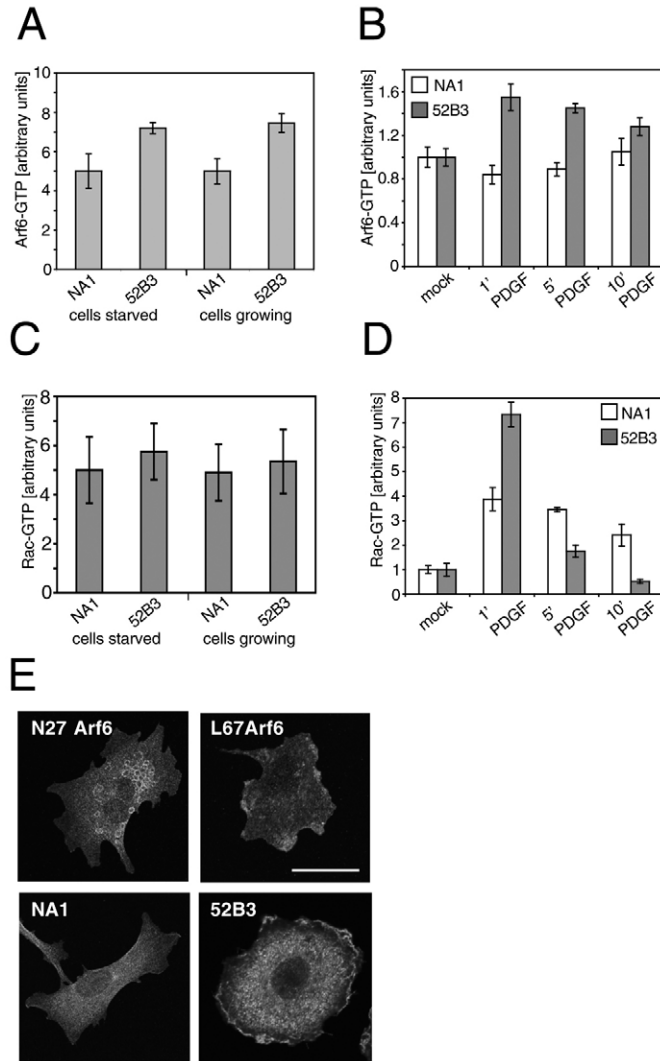
Fig. 5. ARAP3-deficient cells display increased Arf6 and altered Rac activities. (A) NA1 and 52B3 cells were seeded into tissue culture dishes, and either left to grow or subjected to serum starvation for 16 hours as indicated. Cells were lysed and lysates used for Arf 'pull-down' assays using GST-GGA beads as bait. (B) Cells were seeded and starved as in (A) and subsequently stimulated with PDGF or its vehicle for 1, 5 and 10 minutes prior to cell lysis. For ease of comparison, basal levels were adjusted to 1. The graphs shown in (A) and (B) represent pooled data (means ± s.d.) from four independent experiments all of which were carried out in duplicate. (C) NA1 and 52B3 cells were seeded in tissue culture dishes, treated as in (A), and used for Rac 'pull-down' assays using GST PAK-CRIB immobilised on Sepharose beads as bait. The shown graph represents pooled data (means ± s.d.) from four independent experiments. (D) Cells were treated as in (B) and used for Rac 'pull-down' assays; basal levels were again adjusted to 1. The shown graph represents (E) HA-tagged, N27Arf6 or L67Arf6 transfected PAE, NA1 or 52B3 cells (as indicated) were seeded onto pooled data (means ± s.d.) from five independent experiments. (E) HA-tagged, N27Arf6 or L67 Arf6 transfected PAE, NA1 or 52B3 cells (as indicated) onto glass coverslips and serum starved for 16 hours. Cells were fixed, stained using an antibody for Rac1 and visualised by confocal microscopy. Photographed slices were 0.8 μm thick. Bar, 20 μm.

phenotype, which included an altered cell shape, many thin actin stress fibres and an inability to produce lamellipodia in response to PDGF stimulation. In a wound healing assay, ARAP3 RNAi cells again failed to form protrusions and lamellipodia; their ability to polarise was affected. We showed that the ARAP3-knockdown phenotype can be rescued by re-introduction of (human) ARAP3. Furthermore, it could be mimicked by simultaneous overexpression of constitutively active Arf6 and RhoA constructs; both small GTPases contributed to the complex phenotype observed. ARAP3-deficient cells had increased RhoA and Arf6-activities. The timecourse of Rac stimulation and its subcellular localisation were altered in ARAP3-knockdown cells.

Lamellipodia and ruffles

PAE cells have been used as a model system to study the role of PI3K and Rac in PDGF stimulated lamellipodium formation (Wennström et al., 1994; Hawkins et al., 1995). ARAP3 is abundant in PAE cells and its overexpression interfered with lamellipodium formation in PAE cells after PDGF challenge; this depended on both Arf and Rho GAP activities (Krugmann et al., 2002; Krugmann et al., 2004). We show here that depletion of endogenous ARAP3 also interferes with PDGF-induced lamellipodium formation; cells either did not react to PDGF, produced uniform membrane ruffles or dorsal ring ruffles.

We saw dorsal ring ruffles in roughly a third of PDGF stimulated ARAP3 RNAi cells. Ring ruffles have been observed before in a small percentage of growth factor stimulated cells, and this percentage increased dramatically in the ARAP3-deficient cells. PtdIns(3,4,5)P_3, Rac, Ras, Rab5 as well as several Arf6 GAPs have been shown to localise to dorsal ruffles (Buccione et al., 2004 and references therein). While their precise function remains elusive, it is thought they are indicators of the transition from static to motile states. One reason why we saw their increased occurrence in these cells could lie in increased Arf6 activity, since (1) we also observed ring ruffles in PDGF-stimulated PAE cells overexpressing fast

endogenous Rac between an internal pool and localisation at the plasma membrane in PAE cells, with N27Arf6 causing an accumulation of Rac in an internal compartment while L67Arf6 localised a significant amount of Rac to the plasma membrane, even in starved PAE cells. To assess whether ARAP3 RNAi cells are unable to form lamellipodia through an impact on the distribution of Rac, we compared the distribution of endogenous Rac1 in control PAE cells and in 52B3 cells (Fig. 5E, bottom panels). As expected, Rac1 was very predominantly cytoplasmic in serum-starved control cells. However, in serum-starved 52B3 cells, a significant amount of Rac1 was located at the plasma membrane. These results indicate loss of ARAP3 is, regarding Rac1 localisation, equivalent to constitutive activation of Arf6. The failure of ARAP3-deficient cells (and of L67Arf6-expressing cells) to produce protrusive lamellipodia is therefore unlikely to be due to a lack of Rac available for activation at the cell surface.

Discussion

We report here a characterisation of the physiological role of ARAP3 in an endothelial cell model using RNAi-mediated knockdown of ARAP3 expression. We observed a striking

cycling Arf6 and (2) we have shown that in PAE cells, as has been shown before in some other cell types (Radhakrishna et al., 1999; Boshans et al., 2000), Arf6 influences the intracellular localisation of Rac. More Rac was located proximal to or at the plasma membrane in ARAP3-deficient cells and at the same time Rac activation after PDGF stimulation was steeper and faster than in control cells. Assuming this Rac is GDP-loaded, it should be readily available for instant activation after appropriate stimulation. Given that the cells were not capable of making 'normal' lamellipodia (see below), this sudden rush of Rac-GTP may have lead to the increased dorsal ring ruffles we observed.

We also saw membrane ruffling in approximately a third of stimulated ARAP3 RNAi cells. It has previously been shown that cells expressing constitutively active Rac produce membrane ruffling along their entire periphery rather than individual lamellipodia (Ridley et al., 1992). Given that RhoA and Rac can effectively counteract each other (Rottner et al., 1999; Worthylake and Burridge, 2003) and that ARAP3 acts as a GAP on RhoA, it seems likely that a localised inactivation of RhoA is required to allow protrusions to form, which then carry the lamellipodia. Such a view is supported by other findings, such as the recent discovery of Smurf1, a ubiquitin ligase capable of driving proteasomal degradation of RhoA, that is localised in the proximity of forming lamellipodia through its PLCζ-regulated association with the Rac/Cdc42-PAR6 polarity complex (Wang et al., 2003).

Given that we know PDGF causes accumulation of PtdIns(3,4,5)P_3 at the plasma membrane and that this in turn causes the recruitment of several effector proteins, such as Rac GEFs (Welch et al., 2003), certain cytohesin family Arf GEFs (Venkateswarlu and Cullen, 2000) and also ARAP3 (Krugmann et al., 2002), it seems likely, that ARAP3 acts to locally inactivate RhoA and activate Arf6 cycling (in tandem with Arf GEFs). Both of these factors then are prerequisites for successful formation of lamellipodia. Our data describing the impact of ARAP3 depletion on the kinetics of Rac activation support the view that a major role of Arf6 cycling is in the regulation of delivering Rac, however, as described in the introduction, it remains possible that Arf6 has both Rac-dependent and Rac-independent contributions to lamellipodium formation.

In the wound healing assays, we observed again that ARAP3 RNAi cells were incapable of producing normal lamellipodia. While ARAP3 RNAi cells moved at almost the same rate as control RNAi cells, they did so in a less co-ordinated fashion. ARAP3-deficient cells at the edge of the wound formed only delayed protrusions; their microtubules were late at re-organising themselves perpendicular to the wound and polarisation of their golgi apparatus was significantly reduced. It has been shown previously that Rat1 fibroblasts transfected with wt or dominant negative p190RhoGAP constructs were defective in spreading and polarisation of the golgi apparatus (Arthur and Burridge, 2001). These findings complement ours, as fibroblasts are very rich in p190RhoGAP, but not in ARAP3, while PAE cells are rich in ARAP3 but not in p190RhoGAP (data not shown).

It is tempting to speculate from the polarisation defect observed in the wound healing experiments, that ARAP3 RNAi cells might be generally poor at polarisation. In this context it is interesting that ARAP3 expression is highest in peripheral blood leukocytes (Krugmann et al., 2002), cells that move and polarise with exquisite speed and precision in chemotactic gradients. It should therefore prove interesting to establish the dependence of specific cell polarity and movement functions of ARAP3 in more physiological model systems, including whole animal models.

Materials and Methods

Generation of ARAP3 RNAi stable cell lines
PAE cell total RNA was prepared using RNA bee reagent (Tel-Test Inc) according to manufacturer's instructions. cDNA was prepared using reverse transcriptase (Promega). Porcine ARAP3 fragments were generated using PCR with putative pig ARAP3 specific primers (F1 AGGACCTGGACATCGCTGTGTGG, R1 TGTC-AGGTCCAGGCCAAAGTAGATG, F2 TGAGCAGTCTTCAGCCTTGAACA, R2 CCTGGAACTTGTTGTCCTTGCTGCT, F3 CTGTCTGACTACGAGGTGGCTG-AGAAG, R3 TCAGCGGGGAGAACCACTTGCCCAC) as defined from a porcine ARAP3 EST sequence found in the database (BI345913) and from regions of strong conservation between mouse and human ARAP3. The sequenced fragments were analysed according to criteria laid out by Tuschl (Tuschl, 2003) to identify possible RNAi oligos. Five candidates (1-TGCCATCTACTTTGGCCTG; 2-CAGGCACAG-TGCACATCAT; 3-AGGGCTGAAGACAGGCTCA; 4-GCTCTCCCCTCAAGGA-AAC; 5-TGGGAGGAGTCTGATGTAC) were cloned into pSILENCER (Hygro) RNAi expression vectors containing U6 or H1 promoter elements (Ambion). Inserts were verified by sequencing. Down-regulation efficiencies of the five candidate RNAi constructs and of the two promoters were assessed by screening cell lysates of transiently transfected PAE cells by western blotting using the anti-ARAP3 antiserum. Plasmids 'U6-3' and 'U6-5' were potentially effective. PAE cells were transfected with these vectors and a scrambled control (ACTACCGTTGTTATA-GGTG; Ambion) and stable clones selected with hygromycin (0.85 μg/ml; Roche). Lysates of individual clones were screened by western blots with anti-ARAP3 antiserum. Blots were reprobed for loading controls with anti-β-COP.

Cell culture and transfections
PAE RNAi cell lines were routinely cultured in F12 medium supplemented with 10% heat inactivated foetal bovine serum (both Gibco) and 0.45 μg/ml hygromycin (Roche) to keep selective pressure. Cells were starved for 16 hours in Hepes-buffered DMEM containing 1% pre-conditioned medium and 0.45 μg/ml hygromycin. Cells were electroporated as described (Krugman et al., 2002).

Microinjections
Microinjections were performed using an Eppendorf setup (Micromanipulator 5171 and Transjector 5246) with a Zeiss Axiovert 200 microscope. Nuclei of 50-100 serum-starved cells per coverslip were microinjected in 15-20 minutes during which time they were kept in a humidified, temperature- and CO_2-controlled atmosphere. Cells were injected with 0.05 mg/ml plasmid DNA using glass capillaries pulled on a Sutter needle puller; biotin dextran (Molecular Probes) was used as injection marker. Cells were fixed 60-90 minutes after injections.

Immunocytochemistry
Cells were seeded onto coverslips, treated as indicated, and fixed for 10 minutes in 4% paraformaldehyde in PBS. Cells were washed, permeabilised 5 minutes in 0.2% Triton X-100 in PBS, washed again, and quenched with sodium borohydride in PBS. Cells were stained for 1 hour with primary antibodies in PBS, 1% BSA and 30 minutes with alexafluor 488- or 568-coupled secondary antibodies (highly cross-absorbed from Molecular Probes). Weak staining (paxillin, Rac) was boosted by incubation with a tertiary layer of antibody. Microinjected cells were visualised with fluorescein-coupled streptavidin (Molecular Probes). Cells were routinely visualised on an Axiovert2 Zeiss fluorescent microscope with a 63× objective and images acquired using a Diagnostics digital camera. For confocal microscopy, cells were viewed on a Zeiss LSM 510 META microscope with 63× objective and 561 nm laser.

'Pull-down' experiments
2.5×10^6 cells were seeded per 9 cm dish, left to adhere and spread for 5 hours and starved for 16 hours (as indicated). Where indicated, cells were stimulated with PDGF, before being aspirated, washed, scraped and lysates spun. 2% of total lysates were run on a gel to allow visualisation of the total amounts of the GTPases on a blot. The remaining 98% of lysates were subjected to 'pull-down' assays as previously described (Santy and Casanova, 2001; Sander et al., 1998; Nimnual et al., 2003). Western blots were analysed by densitometric scanning using NIH image software.

Rock kinase assays
Cells transiently transfected with pRK5Myc-Rock (kind gift from L. Machesky) or an empty vector control were stimulated with PDGF as indicated, followed by lysis in 50 mM Hepes pH 7.4 at 4°C, 150 mM NaCl, 1 mM Na_3VO_4, 1 mM NaF, 1 mM

PMSF, 1% Triton X-100. Clarified lysates were subjected to BCA protein assay (Pierce), precleared with EE-Sepharose and immunoprecipitated with Myc-Sepharose. After extensive washing, beads were used in a protein kinase assay in a total volume of 40 μl of kinase buffer (10 mM Hepes pH 7.4 at 4°C, 50 mM NaCl, 10 mM MgCl$_2$, 100 μM Na$_3$VO$_4$, 0.5 mM DTT, 25 mM β-glycerophosphate, 2.5 μM ATP, 50 μg/ml MBP). Assays were started by addition of 5.5 μCi γ[^{32}P]ATP (Amersham; 10 mCi/ml) and placing the samples at 30°C for 30 minutes. Assays were stopped by the addition of sample buffer. Proteins were separated on a 12% gel by SDS-PAGE and phosphorylation of MBP was quantified on a phosphoimager (Fuji) using Aida image analyzer software.

MYPT phosphorylation assays

Cells were treated as described for 'pull-down' assays, except that lysis was in 5 mM EGTA, 5 mM EDTA, 20 mM Tris-HCl pH 8.0 at 4°C, 1% NP40, 130 mM NaCl, 10 mM NaF, 20 mM β-glycerophosphate, 0.1 mM Na$_3$VO$_4$, 1 mM PMSF and 10 μg/ml pepstatinA, leupeptin, antipain and aprotinin each. 2% of the precleared cell lysates were loaded onto a 7% SDS-PAGE gel and separated proteins transferred to PVDF (Millipore). Blots were probed for phospho MYPT according to manufacturer's instructions followed by stripping and probing for β-COP to visualise total amounts of proteins loaded.

Antibodies

The previously described anti-ARAP3 antiserum (Krugmann et al., 2002) was immuno-affinity purified. Anti- Rac1 and paxillin were from Transduction Laboratories, anti-Cdc42 (clone P1) and RhoA (clone 26C4) were from Santa Cruz, anti-total MYPT and phospho MYPT (Thr 696) were from Upstate, anti-vinculin, anti-tubulin and rabbit antisera against the Myc and HA tags were from Sigma and anti-GFP was from Clontech. Anti-Arf6 was a gift from S. Bourgoin, anti-giantin from S. Munro and anti-β-COP (clone M3A5) was a gift from N. Ktistakis. Monoclonal antibodies against Phosphotyrosine (4G10), the Myc (9E10) and the HA epitope tags (12CA5) were grown at the antibody facility at the Babraham Institute.

References

Akasaki, T., Koga, H. and Sumimoto, H. (1999). Phosphoinositide 3-kinase-dependent and -independent activation of the small GTPase Rac2 in human neutrophils. *J. Biol. Chem.* **274**, 18055-18059.

Altschuler, Y., Liu, S., Katz, L., Tang, K., Hardy, S., Brodsky, F., Apodaca, G. and Mostov, K. (1999). ADP-ribosylation factor 6 and endocytosis at the apical surface of Madin-Darby canine kidney cells. *J. Cell Biol.* **147**, 7-12.

Amano, M., Chihara, K., Kimura, K., Fukata, Y., Nakamura, N., Matsuura, Y. and Kaibuchi, K. (1997). Formation of actin stress fibers and focal adhesions enhanced by Rho-kinase. *Science* **275**, 1308-1311.

Arthur, W. T. and Burridge, K. (2001). RhoA inactivation by p190RhoGAP regulates cell spreading and migration by promoting membrane protrusion and polarity. *Mol. Biol. Cell* **12**, 2711-2720.

Boshans, R. L., Szanto, S., van Aelst, L. and D'Souza-Schorey, C. (2000). ADP-ribosylation factor 6 regulates actin cytoskeleton remodeling in coordination with Rac1 and RhoA. *Mol. Cell. Biol.* **20**, 3685-3694.

Buccione, R., Orth, J. D. and McNiven, M. A. (2004). Foot and mouth: podosomes, invadopodia and circular dorsal ruffles. *Nat. Rev. Mol. Cell. Biol.* **5**, 647-657.

Cavenagh, M. M., Whitney, J. A., Carroll, L., Zhang, C., Boman, A. L., Rosenwald, A. G., Mellman, I. and Kahn, R. A. (1996). Intracellular distribution of Arf proteins in mammalian cells. Arf6 is uniquely localized to the plasma membrane. *J. Biol. Chem.* **271**, 21767-21774.

Donaldson, J. G. (2003). Multiple roles for Arf6: sorting, structuring, and signalling at the plasma membrane. *J. Biol. Chem.* **278**, 41573-41576.

Franco, M., Peter, P. J., Boretto, J., van Donselaar, E., Neri, A., D'Souza-Schorey, C. and Chavrier, P. (1999). EFA6, a sec7 domain-containing exchange factor for ARF6,

coordinates membrane recycling and actin cytoskeleton organization. *EMBO J.* **18**, 1480-1491.

Hawkins, P. T., Eguinoa, A., Qiu, R. G., Stokoe, D., Cooke, F. T., Walters, R., Wennström, S., Claesson-Welsh, L., Evans, T., Symons, M. et al. (1995). PDGF stimulates an increase in GTP-Rac via activation of phosphoinositide 3-kinase. *Curr. Biol.* **5**, 393-403.

Krugmann, S., Anderson, K. E., Ridley, S. H., Risso, N., McGregor, A., Coadwell, J., Davidson, K., Eguinoa, A., Ellson, C. D., Lipp, P. et al. (2002). Identification of ARAP3, a novel PI3K effector regulating both Arf and Rho GTPases, by selective capture on phosphoinositide affinity matrices. *Mol. Cell* **9**, 95-108.

Krugmann, S., Williams, R., Stephens, L. and Hawkins, P. T. (2004). ARAP3 is a PI3K- and Rap-regulated GAP for RhoA. *Curr. Biol.* **14**, 1380-1384.

Leung, T., Chen, X. Q., Manser, E. and Lim, L. (1996). The p160 RhoA-binding kinase ROKα is a member of a kinase family and is involved in the reorganisation of the cytoskeleton. *Mol. Cell. Biol.* **16**, 5313-5327.

Macia, E., Luton, F., Partisani, M., Cherfils, J., Chardin, P. and Franco, M. (2004). The GDP-bound form of Arf6 is located at the plasma membrane. *J. Cell Sci.* **117**, 2389-2398.

Nimnual, A. S., Taylor. L. J. and Bar-Sagi, D. (2003). Redox-dependent downregulation of Rho by Rac. *Nat. Cell Biol.* **5**, 236-241.

Nobes, C. D., Hawkins, P., Stephens, L. and Hall, A. (1995). Activation of the small GTP binding proteins rho and rac by growth factor receptors. *J. Cell Sci.* **108**, 225-233.

Radhakrishna, H., Al-Awar, O., Khachikian, Z. and Donaldson, J. G. (1999). ARF6 requirement for Rac ruffling suggests a role for membrane trafficking in cortical actin rearrangements. *J. Cell Sci.* **112**, 855-866.

Reif, K., Nobes, C. D., Thomas, G., Hall, A. and Cantrell, D. A. (1996). Phosphatidylinositol 3-kinase signals activate a selective subset of Rac/Rho-dependent effector pathways. *Curr. Biol.* **6**, 1445-1455.

Ridley, A. J. and Hall, A. (1992). The small GTP-binding protein rho regulates the assembly of focal adhesions and actin stress fibers in response to growth factors. *Cell* **70**, 389-399.

Ridley, A. J., Paterson, H. F., Johnston, C. L., Diekmann, D. and Hall, A. (1992). The small GTP-binding protein rac regulates growth factor-induced membrane ruffling. *Cell* **70**, 401-410.

Ridley, A. J., Schwartz, M. A., Burridge, K., Firtel, R. A., Ginsberg, M. H., Borisy, G., Parsons, J. T. and Horwitz, A. R. (2003). Cell migration: integrating signals from front to back. *Science* **302**, 1704-1709.

Rottner, K., Hall, A. and Small, J. V. (1999). Interplay between Rac and Rho in the control of substrate contact dynamics. *Curr. Biol.* **9**, 640-648.

Sander, E. E., van Delft, S., ten Kloster, J. P., van der Kammen, R. A., Michiels, F. and Collard, J. G. (1998). Matrix-dependent Tiam1/Rac signaling in epithelial cells promotes either cell-cell adhesion or cell migration and is regulated by phosphatidylinositol 3-kinase. *J. Cell Biol.* **143**, 1385-1398.

Santy, L. C. (2003). Characterization of a fast cycling ADP-ribosylation factor 6 mutant. *J. Biol. Chem.* **277**, 40185-40188.

Santy, L. C. and Casanova, J. E. (2001). Activation of ARF6 by ARNO stimulates epithelial cell migration through downstream activation of both Rac1 and phospholipase D. *J. Cell Biol.* **154**, 599-610.

Small, J. V., Stradal, T., Vignal, E. and Rottner, K. (2002). The lamellipodium: where motility begins. *Trends Cell Biol.* **12**, 112-120.

Takai, Y., Sasaki, T. and Matozaki, T. (2001). Small GTP-binding proteins. *Physiol. Rev.* **81**, 153-208.

Tuschl, T. (2003). Functional genomics: RNA sets the standard. *Nature* **42**, 220-221.

Vanhaesebroeck, B., Leevers, S. J., Ahmadi, K., Timms, J., Katso, R., Driscoll, P. C., Woscholski, R., Parker, P. J. and Waterfield, M. D. (2001). Synthesis and function of 3-phosphorylated inositol lipids. *Annu. Rev. Biochem.* **70**, 535-602.

Venkateswarlu, K. and Cullen, P. J. (2000). Signalling via ADP-ribosylation factor 6 lies downstream of phosphatidylinositide 3-kinase. *Biochem. J.* **345**, 719-724.

Wang, H. R., Zhang, Y., Ozdamar, B., Ogunjimi, A. A., Alexandrova, E., Thomsen, G. H. and Wrana, J. L. (2003). Regulation of cell polarity and protrusion formation by targeting RhoA for degradation. *Science* **302**, 1775-1779.

Welch, H. C., Coadwell, W. J., Stephens, L. R. and Hawkins, P. T. (2003). Phosphoinositide 3-kinase-dependent activation of Rac. *FEBS Lett.* **546**, 93-97.

Wennström, S., Hawkins, P., Cooke, F., Hara, K., Yonezawa, K., Kasuga, M., Jackson, T., Claesson-Welsh, L. and Stephens, L. (1994). Activation of phosphoinositide 3-kinase is required for PDGF-stimulated membrane ruffling. *Curr. Biol.* **4**, 385-393.

Worthylake, R. A. and Burridge, K. (2003). RhoA and ROCK promote migration by limiting membrane protrusions. *J. Biol. Chem.* **278**, 13578-13584.

Xu, J., Wang, F., van Keymeulen, A., Herzmark, P., Straight, A., Kelly, K., Takuwa, Y., Sugimoto, N., Mitchison, T. and Bourne, H. R. (2003). Divergent signals and cytoskeletal assemblies regulate self-organizing polarity in neutrophils. *Cell* **114**, 201-214.